# Polyolefin blends: 1. Effect of EPR composition on structure, morphology and mechanical properties of HDPE/EPR alloys

**R. Greco, C. Mancarella, E. Martuscelli and G. Ragosta**
*Istituto di Ricerche su Tecnologia dei Polimeri e Reologia del CNR, Arco Felice, 80072 Naples, Italy*

**and Yin Jinghua**
*Changchun Institute of Applied Chemistry, Academia Sinica, China*
*(Received 13 October 1986; revised 4 March 1987; accepted 21 April 1987)*

Differential scanning calorimetry, wide-angle X-ray diffraction, morphology, and mechanical and impact properties of a high-density polyethylene (HDPE)/ethylene–propylene copolymer (EPR) blend (80/20 weight ratio), with the EPR copolymer having various compositions, have been investigated. The results show no evidence of cocrystallization between HDPE and the EPR copolymers even at the highest $C_2$ content. During blend mixing, the copolymers are able to dissolve HDPE low-molecular-weight chains, giving rise to a system with lower crystallinity and higher HDPE crystallite perfection. The observed behaviour is very similar to that of an isotactic polypropylene/ethylene–propylene copolymer studied in a parallel work.

**(Keywords: high density polyethylene; ethylene–propylene copolymers; blends; morphology; mechanical properties)**

## INTRODUCTION

In recent years, the properties of semicrystalline polyolefins, such as low-density polyethylene (LDPE), linear high-density polyethylene (HDPE) and isotactic polypropylene (iPP), blended with ethylene–propylene–diene terpolymer (EPDR) or with ethylene–propylene copolymer (EPR) have been investigated by several authors[1–10]. Generally the above-mentioned copolymer or terpolymer has been used as a toughening agent for polypropylene matrices, especially if coupled with linear polyethylene (HDPE)[3–5]. Therefore a number of investigations have been carried out on the influence of such rubbery polymers on the crystallization behaviour, the morphology and the mechanical properties of iPP[1,4,9–11].

LDPE- or HDPE-based blends, containing EPR or EPDR, have received less attention in the literature, probably because of the minor technological need to toughen them. Therefore fundamental knowledge of these systems in the area of structure–properties relationships is still rather limited. A few EPDR terpolymers were mixed with LDPE and HDPE and the blend properties analysed. Cocrystallization effects were invoked between LDPE and the EPDR having the highest ethylene ($C_2$) content in order to explain the data, whereas a limited mixing for all the EPDRs was observed with HDPE. On lowering the $C_2$ content in the EPDR, the interactions between matrix and rubber were reduced in both cases. Some results on HDPE/EPR[7] and HDPE/EPDR[8] blends have been presented. The whole composition range was investigated using an EPR with a high $C_2$ content in the first work[7] and an EPDR with a lower $C_2$ content in the second one[8]. Mainly morphological influences and limited mixing interactions were found in both cases.

In the present paper a rather systematic study of the influence of EPR composition on the properties of an HDPE/EPR system at a fixed blend ratio (80/20 weight ratio) has been made. The aim is also to compare these results with those relative to a parallel analysis carried out using analogous conditions for iPP/EPR blends[12].

## EXPERIMENTAL

### *Material*

Ethylene–propylene copolymers were synthesized by using the Ziegler–Natta catalyst, $TiCl_3$,$Al(C_2H_5)_2Cl$ (Al/Ti = 4/1). The concentration of the catalyst was 6 mmol $l^{-1}$ (n-heptane solvent). The temperature for the polymerization was 50°C and the polymerization time was an hour. No purification was made thereafter. Copolymers contained long $C_2$ (ethylene) (or $C_3$ (propylene)) sequences along the molecular chain. The characterization of the copolymers is given in *Table 1*: from left to right, the code (letters are an abbreviation of ethylene–propylene (EP) and digits represent the percentage of ethylene in moles), the percentage of ethylene in weight, the feed ratio of monomers to the polymerization reactor, the intrinsic viscosity, the crystallinity $X_c$, the melting temperature $T_m$ and the glass transition temperature $T_g$.

High-density polyethylene, kindly supplied by RAPRA (Rubber and Plastics Research Association of Great Britain), has the following characteristics: $M_w = 1.1 \times 10^5$, $\bar{M}_n = 1.1 \times 10^4$, $M_w/M_n = 10$ and $MFI = 3.7$.

0032-3861/87/111922-07$03.00

**Table 1** Compositions and properties of EPR copolymers

| Code | $C_2$ content (wt%) | Feed ratio of monomers ($C_2/C_3$) | $[\eta]$ (dl $g^{-1}$) in decahydronaphthalene at 135°C) | $X_c$ (%) (d.s.c.) | $T_m$ (°C) | $T_g$ (°C) |
|---|---|---|---|---|---|---|
| EP-84 | 78 | 75/25 | 3.73 | 27 | 125 | −50 |
| EP-69 | 60 | 64/36 | 2.36 | 14 | 126 | −50 |
| EP-59 | 49 | 55/45 | 2.08 | 12 | 125 | −44 |
| EP-45 | 35 | 44/56 | 1.65 | 2 | 123 | −36 |
| EP-12 | 8 | 4/96 | 1.66 | 42 | 143 | 0to −6 |

*Blend preparation*

Blends of HDPE and EPR (the weight ratio is HDPE/EPR = 80/20) were prepared by melt mixing in a Brabender-like apparatus (Haake Rheocord instrument). Blending temperature was 200°C and blending time was 15 min. The rate of the rotor was 32 rpm.

*Specimen preparation*

*Specimens for mechanical tensile tests.* The material obtained by blending was hot-pressed in a hydraulic press (Wabash) at 170°C and about 240 kg $cm^{-2}$. The thickness of the sheets obtained was about 1 mm. Dumbbell specimens were cut from the sheets obtained and used for the mechanical investigations.

*Specimens for d.s.c. experiments.* The following standard procedures were used to prepare specimens for d.s.c. experiments. The specimens were obtained as follows: first the blended samples were heated to 170°C and kept at this temperature for 15 min; then they were quenched at room temperature in water. Fibre specimens were cut from the middle of stretched sample fibres having the same draw ratio of 1200%.

*Specimens for morphology observations.* The thin sections used for optical microscopy were cut cryogenically with an LKB ultramicrotome. Those to be utilized for electron microscopy were cut by using a Reichert-Sung microtome. Some SEM specimens were etched using n-heptane vapour to remove the copolymers. The other SEM specimens were etched with $CrO_3/H_2SO_4$ saturated solution at room temperature for 50 min to destroy the amorphous phase of the blends. The procedure to prepare this kind of solution was as follows: first the concentrated sulphuric acid was diluted with water (the ratio of $H_2SO_4$ to water was 1:4); then it was heated to 80°C and the $CrO_3$ added to form the saturated solution.

*Specimens for fracture tests.* First the blended materials with different HDPE/EPR weight ratios were hot-pressed in the same hydraulic press at 200°C and at a pressure of 240 kg $cm^{-2}$. The moulded sheets obtained were 3.0 mm thick. Then Charpy-type specimens 6.0 mm wide and 6.0 mm long were cut by a mill. Finally all the specimens were notched at the middle of their length as follows: a blunt notch was made by a slotter and then a very sharp notch 0.2 mm deep was produced by a razor blade fixed on a micrometer apparatus. The final value of the notch depth was measured after fracture by using an optical microscope. For the impact studies the following blends were prepared: HDPE/EP-84 and HDPE/EP-45 with 100/0, 90/10, 85/15 and 80/20 (w/w) compositions.

*Techniques*

*Mechanical tensile tests.* Dumbbell specimens were elongated by using an Instron testing machine (at room temperature and at a constant crosshead speed of 10 mm $min^{-1}$). The draw ratio for HDPE and HDPE/EPR blends was about 1200%. Three parameters were calculated from the stress–strain curves: (1) Young's modulus $E$ from the initial slope $(d\sigma/d\varepsilon)_{\varepsilon=0}$; (2) yield strength $\sigma_y$; and (3) constant stress $\sigma_c$ at cold-drawing.

Fibres were cut from stretched specimens between the two necks at a length of 5 cm and were redrawn by the same testing machine (at room temperature and at constant crosshead speed of 10 mm $min^{-1}$). From stress–strain curves were calculated the following: (1) Young's modulus $E$; (2) tensile strength $\sigma_b$; and (3) elongation at break $\varepsilon_b$.

*D.s.c. measurements.* Crystallinity $X_c$, melting temperature $T_m$, crystallization temperature $T_c$ and widths at half height of the melting and crystallization peaks for the d.s.c. specimens mentioned earlier were determined by using a Mettler TA 3000 system apparatus. The rate of increasing and decreasing the temperature was 20 K $min^{-1}$. For the determination of $T_c$ the samples were kept for 10 min at 200°C. The weight of the specimens was about 7 mg.

*Morphology observations.* Optical micrographs were taken by using a Wild M420 microscope. The surfaces of the specimens observed by SEM were coated with Au–Pd and observed by a Philips 501 B scanning electron microscope.

*WAXD measurements.* Wide-angle X-ray diffraction measurements were performed by means of a Philips PW 1060/71 diffractometer with Ni-filtered Cu Kα radiation. The high voltage was 50 kV and the tube current was 30 mA.

*Impact fracture measurements.* Charpy impact tests were carried out at an impact speed of 1 m $s^{-1}$ by using a Ceast fracture pendulum. Samples with a notch depth-to-width ratio of 0.3 and a span test of 48 mm were fractured at different temperatures ranging from −100 up to 20°C. The temperature was changed by means of a home-made liquid-nitrogen apparatus. Curves of the impact strength as a function of the test temperature were obtained for all the HDPE/EP-84 and HDPE/EP-45 blends.

## RESULTS AND DISCUSSION

*Unoriented specimens*

*Morphology.* Optical micrographs with crossed polars of thin films of HDPE, HDPE/EP-84 and HDPE/EP-12 blends are reported in *Figure 1*. The nucleating influence of the EP-84 and EP-12 copolymers on HDPE is clearly demonstrated by comparing the micrographs, since a heterogeneous nucleation effect due to inclusions or added nucleants can be excluded by indirect evidence.

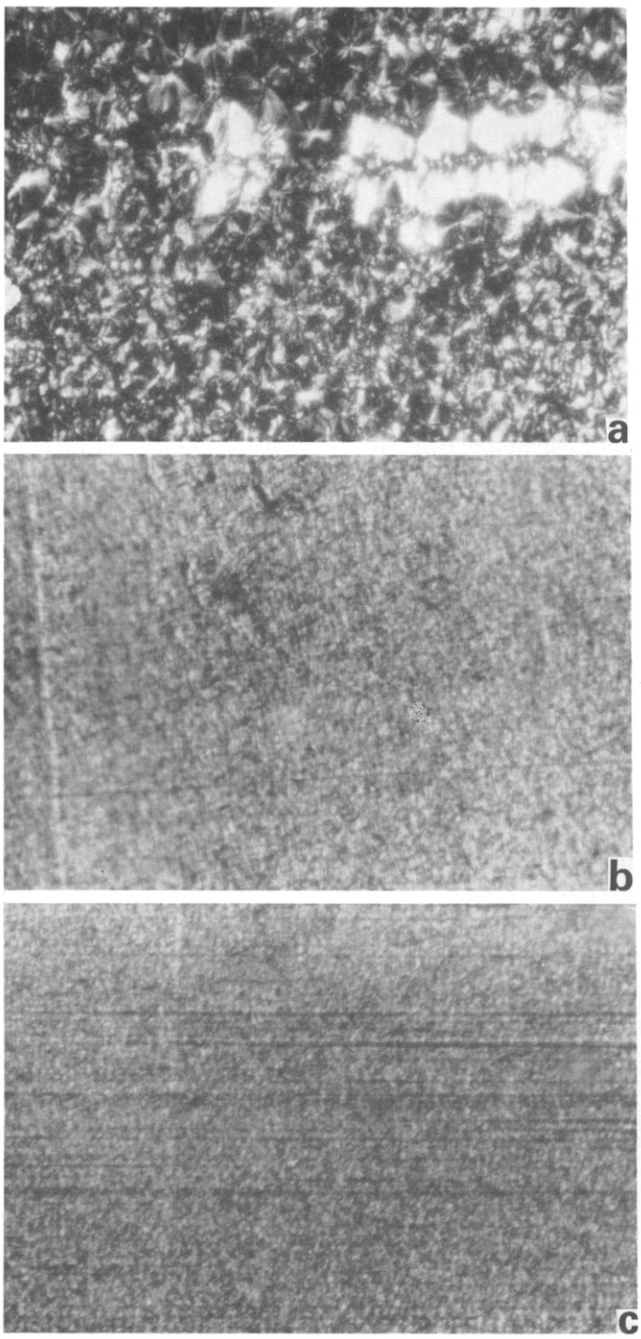


**Figure 1** Optimal micrographs (150×) at crossed polars of thin sections: (a) HDPE; (b) HDPE/EP-80; (c) HDPE/EP-12

In the third paper of this series[13], for blends crystallized at a low undercooling, this effect on the iPP matrix did not always occur. It depended, instead, only on the $C_2$ content of the copolymers. This result tends therefore to indicate that, even though the copolymers were not purified after synthesis, the eventual impurities have a negligible influence on iPP nucleation. If this holds for iPP matrices[12,13], in HDPE ones also the nucleation will depend only on the rubber's action.

Electron micrographs of smoothed surfaces, etched with n-heptane, are shown in *Figures 2–7*. Going from the pure HDPE (*Figure 2*) and progressively decreasing the $C_2$ content in the added copolymers (from *Figure 3* to *Figure 7*) it was possible to extract more and more amorphous material from the surface by dissolving in boiling n-heptane. In fact the holes increase in size more and more, indicating a diminution of compatibility in the amorphous regions between the HDPE matrix and the copolymers.

A different etch with strong oxidants ($CrO_3/H_2SO_4$) revealed the spherulitic structure and some details of the

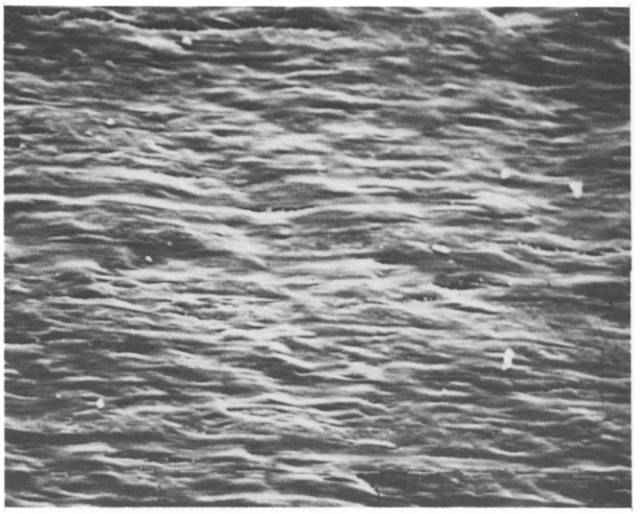

**Figure 2** Electron micrographs (3600×) of a smoothed HDPE sample surface etched for 15 min with boiling n-heptane vapour

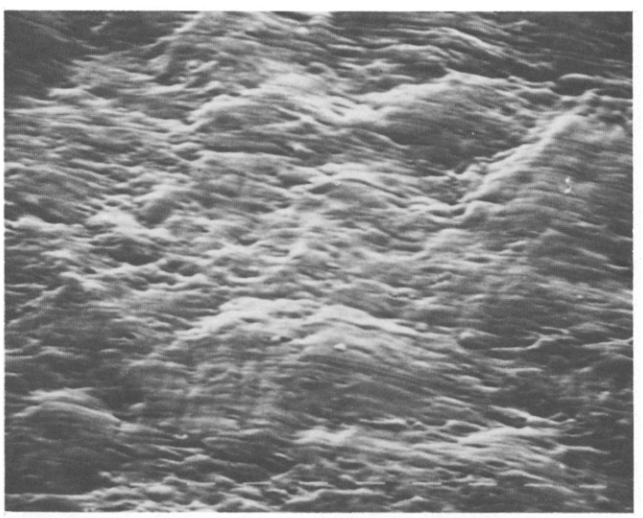

**Figure 3** Scanning electron micrograph (3600×) of a smoothed HDPE/EP-84 sample surface etched for 20 min with boiling n-heptane vapour

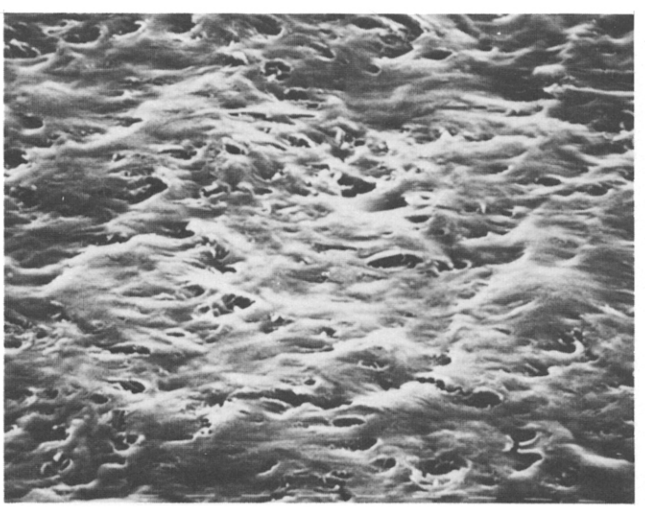

**Figure 4** Scanning electron micrograph (3600×) of a smoothed HDPE/EP-69 sample surface etched for 10 min with boiling n-heptane vapour

lamellar structure by attack of all the amorphous regions of both HDPE and the copolymers. This is shown in *Figure 8* for HDPE, in *Figure 9* for EP-84 and in *Figure 10* for EP-69. For HDPE/EP-84 and HDPE/EP-69 blends the spherulites looked more open since there was more amorphous content to be destroyed among spherulites and lamellae.

*Thermal properties.* The parameters calculated from the differential scanning thermograms are reported for

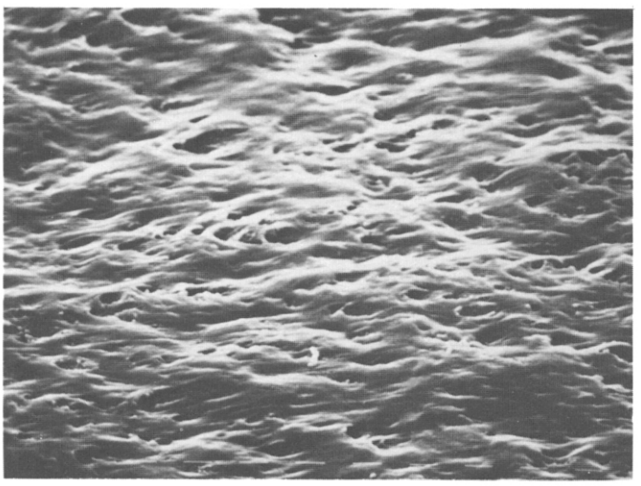

**Figure 5** Scanning electron micrograph (3600×) of a smoothed HDPE/EP-59 sample surface etched for 10 min with boiling n-heptane vapour

**Figure 6** Scanning electron micrograph (3600×) of a smoothed HDPE/EP-45 sample surface etched for 1.5 min with boiling n-heptane vapour

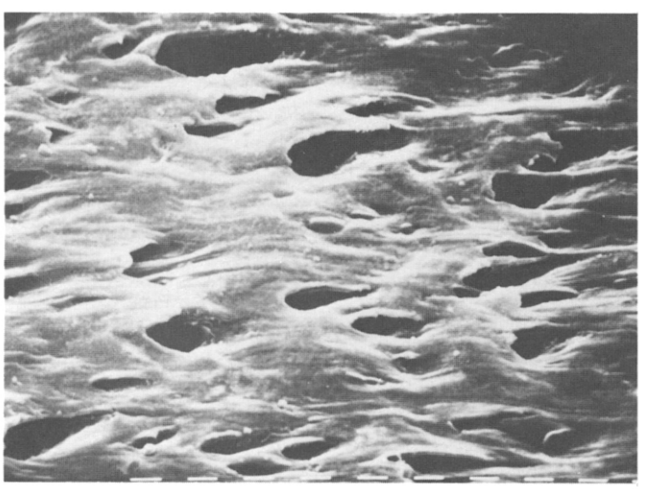

**Figure 7** Scanning electron micrograph (3600×) of a smoothed HDPE/EP-12 sample surface etched for 3 min with boiling n-heptane vapour

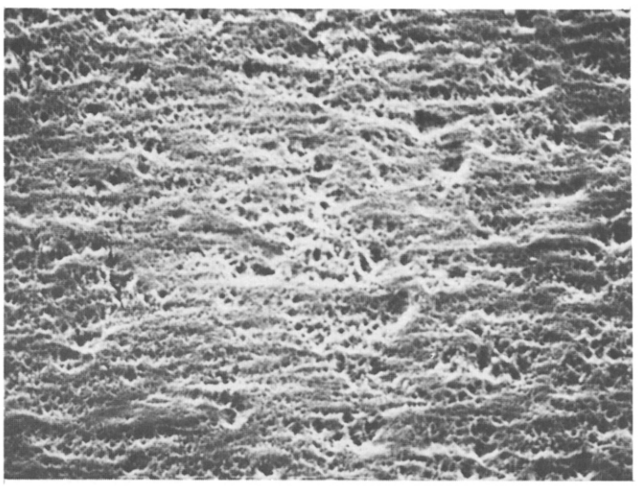

**Figure 8** Scanning electron micrograph (3600×) of a smoothed HDPE sample surface etched by a strong oxidant mixture (for details see text) for 90 min

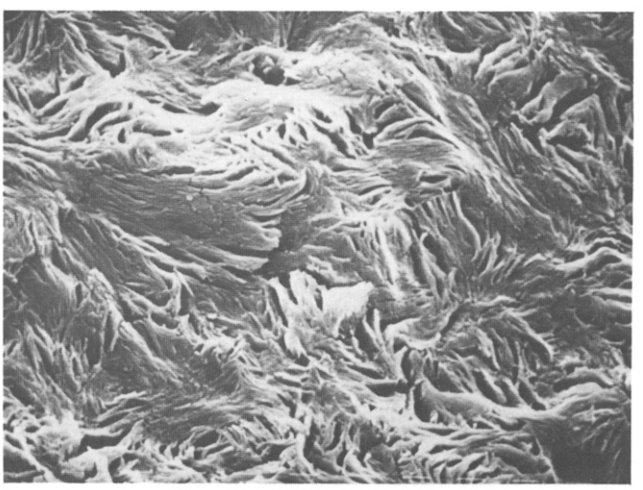

**Figure 9** Scanning electron micrograph (3600×) of a smoothed HDPE/EP-84 sample surface etched by an oxidant mixture (for details see text) for 150 min

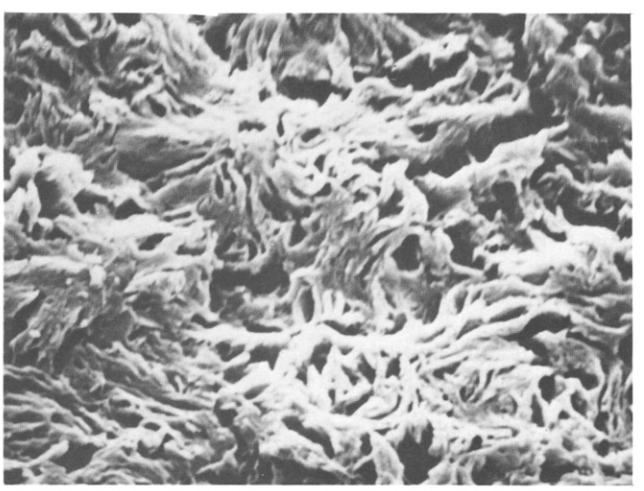

**Figure 10** Scanning electron micrograph (3600×) of a smoothed HDPE/EP-69 sample surface etched by an oxidant mixture (for details see text) for 150 min

**Table 2** Crystallinity, melting temperature $T_m$, crystallization temperature $T_c$ and width at half height of $T_m$ and $T_c$ peaks for HDPE/EPR blends

| Sample | Crystallinity (%) | | Melting temperature (°C) | Crystallization temperature (°C) | Width at half height of peak (K) | |
|---|---|---|---|---|---|---|
| | $X_c$ | $X_c^p$ | | | $T_m$ peak | $T_c$ peak |
| HDPE | 79 | 79 | 137 | 111 | 19 | 20 |
| HDPE/EP-84 | 60 | 68 | 142 | 114 | 17 | 17 |
| HDPE/EP-69 | 55 | 66 | 141 | 114 | 17 | 17 |
| HDPE/EP-59 | 52 | 65 | 141 | 115 | 18 | 17 |
| HDPE/EP-45 | 50 | 64 | 141 | 114 | 18 | 17 |
| HDPE/EP-12 | 59 | 71 | 148 | 114 | 19 | 18 |

pure HDPE and for all the HDPE/EPR (80/20) blends in *Table 2*: from left to right, the type of blend, the measured overall crystallinity $X_c$, the crystallinity $X_c^p$ (calculated assuming no HDPE–EPR interaction from the equation $X_c^p = W_{HDPE}X_{HDPE} + W_{EP}X_{EP}$ where $W$ and $X$ are the relative weight ratios and crystallinities, between the polyolefin and the copolymer), the melting and crystallization temperatures $T_m$ and $T_c$ and the width at half height of the melting and crystallization peaks are shown.

The overall crystallinity $X_c$ decreases for all the blends with respect to the pure HDPE. This can be due partly to the substitution of 20% HDPE with less crystalline copolymers. But $X_c$ is lower than $X_c^p$, indicating that there is a certain amount of interaction between HDPE and EPR during crystallization.

This effect is also confirmed by the fact that the melting and crystallization temperatures $T_m$ and $T_c$ are higher for the blends than for the homopolymer. A further complementary observation is the width at half height of the $T_m$ and $T_c$ peaks, which are narrower for the blends than for the HDPE.

All these features could be tentatively explained as follows. During the melt-mixing in the Brabender-like apparatus the copolymers were able to dissolve HDPE defective molecules (i.e. of lower molecular weight). Therefore during pressure moulding and the successive rapid crystallization this segregation between high-molecular-weight HDPE and the new HDPE/copolymer phase containing defective HDPE chains was still retained. Hence more perfect crystals (high $T_m$ and $T_c$) and a narrower distribution of lamellae or crystallite dimensions (lower width at half height of $T_m$ and $T_c$ peaks) for the blends than for pure HDPE were obtained. The behaviour of the last blend (HDPE/EP-12) should be analysed more carefully since it contains two crystalline phases, the HDPE one and the $C_3$ crystallites, as will be shown later also by wide-angle X-ray scattering measurements. In fact the melting and crystallization peaks of HDPE also contain the $C_3$ crystallite contribution, which cannot be evaluated. This effect can, at least partially, explain the even higher $T_m$ and the broader peak in comparison to that of all other blends.

*X-ray diffraction.* Wide-angle X-ray scattering (WAXS) patterns are shown in *Figure 11*, where the intensities in arbitrary units are plotted against the diffraction angle $2\theta$. As shown the blend HDPE/EP-84 reveals the same pattern as pure HDPE, whereas the HDPE/EP-12 blend also contains $C_3$ crystallites, indicating that its $X_c$ (*Table 2*) has been overestimated. This finding confirms the substantial incompatibility in the solid EP-12 copolymer and the better compatibility of the other ones with the

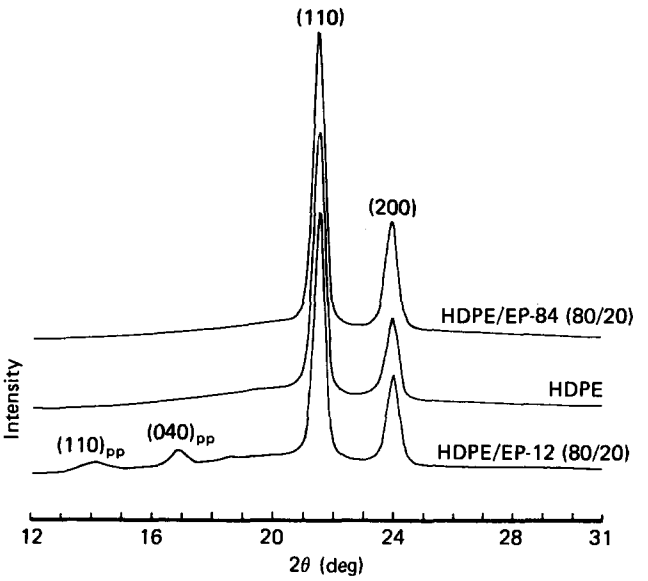


**Figure 11** Wide-angle X-ray diffraction intensity as a function of diffraction angle $2\theta$ for HDPE and blends

HDPE matrix, evidenced by the morphology of the etched specimens (*Figures 2–7*).

*Mechanical properties.* The Young's modulus $E$, the yield stress $\sigma_y$ and also the stress at cold-drawing $\sigma_c$ are reported in *Table 3* for all the investigated blends. All of them exhibit the same trend with a minimum at $C_2$ of about 50%. There is no $\sigma_c$ value for the HDPE/EP-12 blend since its specimens broke before cold-drawing due to the gross morphology of the EP-12 dispersed phase (see *Figure 7*).

The analogous trends of $E$ and $\sigma_y$ can be explained as follows. In the range of $C_2$ from 40 to 100% in the copolymers up to pure HDPE there is an increase of crystallinity from 50 to 79% (see *Table 2*). Moreover, the glass transition temperature of HDPE and also of the copolymers is far below room temperature (see *Table 1*), at which the mechanical tensile tests have been performed. Therefore $E$ and $\sigma_y$ follow an increasing trend with enhancing $C_2$ content of the EPR copolymers.

If one considers now the HDPE/EP-12 blend one can see, from the above-mentioned tables, that its crystallinity content is a little higher with respect to all the other blends. But what is more significant is that its glass transition temperature (0–6°C) is lower than the test temperature (20°C). This tends to increase the $E$ and $\sigma_y$ values, which become comparable to that of pure HDPE. A further consideration is that for this last blend there is a strong segregation of the copolymer from the matrix in semicrystalline glassy particles.

**Table 3** Young's modulus $E$, tensile yield stress $\sigma_y$ and cold-drawing constant stress $\sigma_c$ of HDPE and HDPE/EPR blends

| Sample | Composition (HDPE/EPR in weight) | $C_2$ content of EPR (wt%) | $E \times 10^{-3}$ (kg cm$^{-2}$) | $\sigma_y \times 10^{-2}$ (kg cm$^{-2}$) | $\sigma_c \times 10^{-2}$ (kg cm$^{-2}$) |
|---|---|---|---|---|---|
| HDPE | 100/0 | – | 11.3 | 3.2 | 2.0 |
| HDPE/EP-84 | 80/20 | 78 | 8.5 | 2.5 | 1.7 |
| HDPE/EP-69 | 80/20 | 60 | 7.5 | 2.2 | 1.4 |
| HDPE/EP-59 | 80/20 | 49 | 7.4 | 2.0 | 1.4 |
| HDPE/EP-45 | 80/20 | 35 | 7.2 | 2.0 | 1.3 |
| HDPE/EP-12 | 80/20 | 8 | 11.0 | 3.1 | – |

There are in fact long $C_3$ sequences in chains which are rejected by the growing fronts of the HDPE spherulites. These large dispersed hard domains strongly hamper matrix cold-drawing and cause premature rupture before fibre formation. This effect is evidenced by the morphology observations already mentioned above.

*Impact properties.* The impact strength ($R$) obtained by Charpy tests as a function of temperature is reported in *Figure 12* for HDPE homopolymer and for all the HDPE/EP-45 and HDPE/EP-69 blends. As can be seen, at low temperatures up to about −40°C, the impact data of pure HDPE remain constant at low values and the corresponding fracture surfaces exhibit features characteristic of a brittle material. As the temperature rises the impact strength begins to increase and the appearance of a stress-whitening zone near the base of the notch, which increases in extent with enhancing temperature, can be observed.

The addition of a copolymer (EP-45 or EP-69) produces in the region of low temperatures a lowering of the impact strength due essentially to the fact that the rubber particles behave as hard fillers and their adhesion to the surrounding matrix is very poor. Thereafter at test temperatures beyond −20°C for PE/EP-45 blends and 0°C for PE/EP-69 blends a sharp rise in the $R$ values is detected, being higher for greater amounts of copolymer. This enhancement, which is larger in the case of PE/EP-45 alloys, is accompanied by a diffuse stress-whitening phenomenon over the entire fracture surface.

The lower toughening action observed for EP-69 with respect to the EP-45 copolymer can probably be ascribed to its higher crystallinity content, which renders the EP-69 domains more rigid and therefore less effective in controlling the craze propagation process in the HDPE matrix.

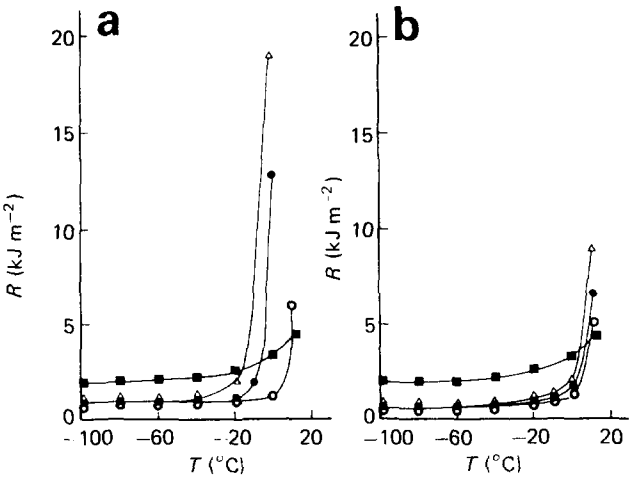


**Figure 12** Resilience $R$ as a function of testing temperature: (a) curves for HDPE/EP-45 blends at various EP-45 contents: ■, 0%; ○, 10%; ●, 15%; △, 20%; (b) curves for HDPE/EP-69 blend at various EP-69 contents: ■, 0%;; ○, 10%; ●, 15%; △, 20%

**Table 4** Crystallinity, melting temperature and width at half height of melting peak for fibres of HDPE and HDPE/EPR blends

| Sample | Crystallinity (%) | Melting temperature (°C) | Width at half height of melting peak (K) |
|---|---|---|---|
| HDPE | 79 | 140 | 13 |
| HDPE/EP-84 | 68 | 140 | 13 |
| HDPE/EP-69 | 65 | 139 | 13 |
| HDPE/EP-59 | 64 | 139 | 14 |
| HDPE/EP-45 | 63 | 139 | 14 |

*Fibres*

*Thermal properties.* The parameters of fibres, i.e. overall crystallinity $X_c$, melting temperature $T_m$ and width at half height of $T_m$ peak, are reported in *Table 4*. Comparison of *Table 4* with *Table 3* shows that the crystallinity of HDPE fibres has remained unchanged with respect to the initial unoriented material, whereas the melting point is increased. This indicates that some local melting and recrystallization under stress has improved crystal perfection and probably also that they are less polydispersed in size (the width at half height of the melting peak is lower for fibres).

Instead for the blends the $T_m$ of fibres is slightly lower, whereas the crystallinity content $X_c$ is considerably higher with respect to the unoriented samples. This seems to suggest that here also some local melt mixing and recrystallization has occurred during cold-drawing into the neck. Therefore the segregation effect between the HDPE and the copolymers is not so sharp as before. Of course the HDPE blend matrix improves its crystal perfection as well as pure HDPE.

*Tensile properties.* The Young's modulus $E$, the tensile strength $\sigma_b$ and the elongation at break $\varepsilon_b$ are reported in *Table 5*. For $E$ and $\sigma_b$ there is a sharp increase with $C_2$ increase, probably due to the enhanced crystallinity content (see *Table 5*). During the morphological transformation, in fact, from the microspherulitic structure to the fibrillar one, $X_c$ is higher the larger the number of taut tie molecules that bridge the fibrils formed during cold-drawing. Hence $E$ and $\sigma_b$ increase with increasing $C_2$ content. The elongation at break $\varepsilon_b$, in contrast, decreases, showing a minimum value for pure HDPE. This is still due to the more rigid structure built on a material structured on a higher crystallinity content.

**Table 5** Young's modulus $E$, tensile strength $\sigma_b$ and elongation at break $e_b$ of HDPE and HDPE/EPR fibres

| Sample | Composition (HDPE/EPR in weight) | $C_2$ content of EPR (wt%) | $E \times 10^{-3}$ (kg cm$^{-2}$) | $\sigma_b \times 10^{-2}$ (kg cm$^{-2}$) | $\varepsilon_b$ (%) |
|---|---|---|---|---|---|
| HDPE | 100/0 | – | 42.4 | 26.1 | 31 |
| HDPE/EP-84 | 80/20 | 78 | 20.2 | 17.0 | 39 |
| HDPE/EP-69 | 80/20 | 60 | 19.2 | 16.8 | 44 |
| HDPE/EP-59 | 80/20 | 49 | 20.2 | 16.9 | 45 |
| HDPE/EP-45 | 80/20 | 35 | 12.1 | 12.2 | 45 |

## CONCLUSIONS

The influence of copolymer composition on the properties of HDPE/EPR blends having a fixed composition (80/20 weight ratio) have been extensively analysed. In particular the following conclusions can be drawn:

(1) The nucleating effect of the copolymers on the HDPE matrix has been observed by optical microscopy.

(2) The compatibility between HDPE and the copolymer increases with increasing $C_2$ copolymer content.

(3) Higher melting points and lower crystallinity content are obtained for the blends with respect to pure HDPE.

(4) The mechanical properties ($E$, $\sigma_y$ and $\sigma_c$) of unoriented specimens decrease with decreasing $C_2$ content in the blends. An exception must be made for the HDPE/EP-12 blend due to the presence of $C_3$ crystallites (as shown by WAXS), which act as reinforcing elements. For fibres $E$ and $\sigma_b$ decrease and $\varepsilon_b$ increases with decreasing $C_2$.

(5) The impact properties improve slightly for the blends and are better in the case of lower compatibility between HDPE and the copolymer used.

The above results are very similar to those found in a parallel work for iPP-based blends with EPR at different $C_3$ contents.

## ACKNOWLEDGEMENTS

The authors wish to thank Mr L. Serio, Mr V. D. Liello and Mr M. Viola for their help in carrying out the experimental work.

## REFERENCES

1 Karger-Kocsis, J., Kallo', A., Szafner, A., Boder, G. and Sényei, Z. *Polymer* 1979, **20**, 37
2 Starkweather, H. W. Jr, *J. Appl. Polym. Sci.* 1980, **25**, 139
3 Stehling, F. C., Huff, T., Speed, C. S. and Wissler, G. *J. Appl. Polym. Sci.* 1981, **26**, 2695
4 Martuscelli, E., Silvestre, C. and Abate, G. *Polymer* 1982, **23**, 229
5 D'Orazio, L., Greco, R., Mancarella, C., Martuscelli, E., Ragosta, G. and Silvestre, C. *Polym. Eng. Sci.* 1982, **22**, 536
6 D'Orazio, L., Greco, R., Martuscelli, E. and Ragosta, G. *Polym. Eng. Sci.* 1982, **23**, 489
7 Kalfoglou, N. K. *J. Macromol. Sci.* 1983, **B22**, 343
8 Kalfoglou, N. K. *J. Macromol. Sci.* 1983, **B22**, 363
9 Karger-Kocsis, J., Kiss, L. and Kuleznev, V. N. *Polym. Commun.* 1984, **25**, 122
10 Karger-Kocsis, J., Kallo', A. and Kuleznev, V. N. *Polymer* 1984, **25**, 279
11 Barkczak, Z., Galeski, A. and Martuscelli, E. *Polym. Eng. Sci.* 1984, **24**, 1155
12 Greco, R., Mancarella, C., Martuscelli, E., Ragosta, G. and Jinghua, Y. *Polymer* 1987, **28**, 1929
13 Greco, R., Martuscelli, E., Ragosta, G. and Jinghua, Y. *Polymer* submitted for publication